Nigerian Journal of Pharmaceutical and Applied Science Research,
Vol.15 (2): 7-22; June 2026 ISSN: 2971-737X (Print); ISSN: 2971-7388.
Available at www.nijophasr.net https://doi.org/10.60787/nijophasr-v15-i2-649

In Silico Evaluation of the Antidiarrhoeal Potential of Phytoconstituents from *Vernonia amygdalina*, *Ocimum gratissimum* and *Piper guineense*.

[1*]Uyi M. Ogbeide and [2]Kluvet O. Owowenu

[1]Department of Pharmaceutical Chemistry, Faculty of Pharmacy, University of Benin, Benin City, Edo State, Nigeria.
[2]Damilola Pharmacy, 2 Ahmed Bola Tinubu Way, off Station, Bust Stop, Fagba, Iju, Lagos.

Article info: Volume 15, Issue 2, June 2026; Received: May 21, 2026; Reviewed: June 1, 2026, Accepted: June 5, 2026; Published: June 15, 2026; *DOI: 10.60787/nijophasr-v14-i2-649*

ABSTRACT

Background: Diarrhoeal diseases remain a major global public health concern, especially in developing countries where access to affordable and effective treatment is limited. This study evaluates the antidiarrhoeal potential of phytochemicals from *Vernonia amygdalina*, *Ocimum gratissimum*, and *Piper guineense* using molecular docking and pharmacokinetic prediction.

Methods: Identified bioactive compounds were docked against two diarrhoeal-related molecular targets: the mu-opioid receptor (PDB ID: 6DDF) and the human serotonin transporter (PDB ID: 6DZZ), alongside standard antidiarrhoeal drugs. Binding affinity scores and ligand–receptor interactions were analyzed to assess inhibitory potential, while drug-likeness and ADME properties were evaluated to determine pharmacokinetic suitability.

Results: Several phytoconstituents showed strong binding affinities comparable to standard drugs and formed stable interactions with key active-site residues in both target proteins. Pharmacokinetic analysis indicated that many compounds satisfied drug-likeness criteria and exhibited favorable oral bioavailability profiles.

Conclusion: The findings suggest that phytochemicals in these commonly consumed vegetables may influence molecular pathways involved in intestinal motility and secretion, supporting their traditional dietary and therapeutic relevance in diarrhoeal management. These compounds may serve as promising leads for the development of plant-based antidiarrhoeal agents.

Keywords: Antidiarrhoeal activity, Drug-likeness, Ligands, Phytochemicals, Serotonin.

1.0 INTRODUCTION

Diarrhoeal disease remains a major public health concern globally, particularly in low- and middle-income countries where it contributes substantially to morbidity and mortality among children under five years of age. It is characterized by the passage of loose or watery stools arising from disturbances in intestinal absorption, secretion, and motility, often triggered by infectious agents and inflammatory processes. Despite advances in sanitation and oral rehydration therapy, diarrhoeal diseases continue to rank among the leading causes of preventable deaths worldwide [1]. The growing burden of antimicrobial resistance among enteric pathogens further complicates therapeutic outcomes and highlights the need for alternative strategies that complement conventional antimicrobial interventions. Key mechanisms in diarrhoeal pathophysiology involve dysregulation of gastrointestinal motility and secretory processes. The μ-opioid receptor (MOR) is a well-established pharmacological target because its activation reduces intestinal peristalsis, inhibits fluid secretion, and enhances water absorption within the gut [2,3]. Loperamide, a peripheral MOR

*corresponding author: Email: uyi.ogbeide@uniben.edu; Phone: +2347038058676

agonist, remains the standard antidiarrhoeal agent due to its ability to slow intestinal transit without central nervous system effects [3]. Structural elucidation of the active-state human MOR–Gi protein complex provides high-resolution insight into ligand-binding pockets and receptor activation mechanisms, supporting structure-based drug discovery efforts aimed at identifying compounds with antidiarrhoeal potential [4]. Although originally resolved for studies of opioid signaling, the receptor's direct role in regulating gastrointestinal motility provides strong biological justification for its inclusion *in silico* investigations targeting diarrhoeal disease. Alterations in gastrointestinal serotonin signaling also contribute to diarrhoeal pathophysiology. Serotonin regulates intestinal motility and secretion, and excessive serotonergic activity has been associated with accelerated transit and increased fluid loss [5]. The serotonin transporter (SERT) modulates extracellular serotonin levels by mediating its reuptake, thereby influencing gut motility and secretory responses. High-resolution structural data for the human serotonin transporter (PDB ID: 6DZZ), resolved in complex with ibogaine and Fab fragments, reveal detailed ligand-binding sites and conformational states relevant to transporter function [6]. This structural information supports molecular docking approaches aimed at identifying compounds capable of modulating SERT activity, providing an indirect but mechanistically plausible strategy for influencing gastrointestinal function in diarrhoeal conditions [5]. Although SERT is not a classical antidiarrhoeal target, its role in serotonin-mediated gut regulation justifies exploration of phytochemical interactions with this protein in computational drug discovery studies. Medicinal plants remain an important resource for managing gastrointestinal disorders in many African communities. In Nigeria, botanicals such as *Vernonia amygdalina, Ocimum gratissimum*, and *Piper guineense* components of traditional dietary preparations—are employed ethnomedicinally for diarrhoeal management. These plants contain bioactive phytochemicals including flavonoids, terpenoids, and phenolic compounds with antimicrobial, antioxidant, and anti-inflammatory properties that may ameliorate diarrhoeal symptoms [7,8]. *Vernonia amygdalina* exhibits antimicrobial and anti-inflammatory activities attributed to sesquiterpene lactones and steroidal saponins, which may support intestinal mucosal protection [9]. *Ocimum gratissimum* essential oils rich in eugenol and thymol demonstrate antimicrobial and antispasmodic effects against enteric pathogens [7], while *Piper guineense* contains piperine and related phenolic compounds with antioxidant properties that may reduce oxidative stress in the gastrointestinal tract [8] Despite these pharmacological observations, molecular evidence regarding interactions between phytochemicals and validated diarrhoeal targets remains limited. Advances in computational pharmacology facilitate early-stage evaluation of plant-derived compounds through molecular docking and *in silico* pharmacokinetic assessment. Docking studies enable prediction of ligand–protein interactions and binding affinities using three-dimensional structural models, providing mechanistic insight prior to experimental validation [10]. The availability of structural data for gastrointestinal regulatory proteins and serotonin transporters supports structure-based drug discovery strategies aimed at identifying novel antidiarrhoeal candidates [6]. Therefore, this study employs molecular docking and pharmacokinetic prediction to evaluate phytochemicals from *Vernonia amygdalina*, *Ocimum gratissimum*, and *Piper guineense* against relevant gastrointestinal targets. The findings are expected to provide scientific support for traditional medicinal practices and contribute to the discovery of plant-derived compounds with therapeutic potential for diarrhoeal disease management in alignment with the research objectives. Therefore, this study aimed to evaluate the *in silico* antidiarrhoeal potential of phytoconstituents from *Vernonia amygdalina, Ocimum gratissimum,* and *Piper guineense* using molecular docking and pharmacokinetic prediction approaches.

2.0 MATERIALS AND METHODS

2.1 Materials

2.1.1 Biological Materials

Vernonia amygdalina, Ocimum gratissimum, Piper guineense

2.1.2 Chemicals and Reagents

Computer databases/web resources were used

2.1.3 Equipment and Other Materials

PyRx, AutoDock Vina, Discovery Studio, PyMOL, SwissADME, ADMETLAB, computer with the following specifications: 64-bit Windows 10 operating system equipped with an Intel® Core™ i5 processor and 32 GB Random Access Memory (RAM).

2.2 Methods

2.2.1 Collection and Preparation of Phytochemicals:

Phytochemical constituents of *Vernonia amygdalina*, *Ocimum gratissimum*, and *Piper guineense* were identified from recent peer-reviewed literature (2016–2024) and validated using the PubChem database. The three-dimensional (3D) structures of selected bioactive compounds were retrieved from PubChem in SDF format [12]. Ligand preparation, including energy minimization and format conversion to PDBQT, was performed using PyRx 0.8 with the Open Babel interface. Energy minimization was carried out using the Universal Force Field (UFF) to obtain stable conformations suitable for docking analysis.

2.2.2 Preparation of Protein Targets

The crystal structures of the two target receptors with Protein Data Bank (PDB) IDs 6DDF (Mu Opioid Receptor-Gi Protein Complex) and 6DZZ (Cryo-EM Structure of the wild-type human serotonin transporter in complex with ibogaine and 15B8 Fab in the inward conformation) were retrieved from the RCSB Protein Data Bank [13]. Protein preparation was conducted using AutoDock Tools integrated within the PyRx environment. Co-crystallized ligands, water molecules, and other heteroatoms were removed, while polar hydrogen atoms were added to the protein structures to ensure proper electrostatic interactions. The prepared receptors were saved in PDBQT format for docking analysis.

2.2.3 Docking Validation and Accuracy Assessment:

The molecular docking protocol was validated through a re-docking (self-docking) procedure to assess the reliability and predictive accuracy of the docking method employed. Docking validation is essential in molecular docking studies because it confirms whether the selected docking parameters can accurately reproduce the experimentally observed binding orientation of a ligand within the receptor binding pocket [15,16]. The co-crystallized ligands associated with the target proteins, 6DDF (μ-opioid receptor–Gi protein complex) and 6DZZ (human serotonin transporter), were extracted from their respective protein structures prior to docking. The prepared receptors were subjected to the same docking conditions used for the phytoconstituents, including identical grid box dimensions, exhaustiveness settings, and scoring parameters within the AutoDock Vina algorithm integrated in PyRx. The extracted native ligands were subsequently re-docked into their original binding pockets to evaluate docking accuracy. Validation was assessed by comparing the predicted binding poses with the experimentally resolved crystallographic conformations using root mean square deviation (RMSD) analysis. RMSD values of ≤ 2.0 Å are generally considered indicative of acceptable docking accuracy and successful reproduction of ligand binding orientation [15,16]. The re-docking results showed close agreement between the predicted and crystallographic binding poses of the native ligands within the active sites of both receptors. In addition, key amino acid residues involved in receptor activity, including **ASP147** for the μ-opioid receptor and **ASP98** and **PHE335** for the serotonin transporter, remained conserved during ligand interaction analysis. These findings confirmed the suitability and reliability of the docking protocol for screening phytoconstituents against the selected diarrhoeal-related molecular targets**.**

*2.2.4 Molecular Docking Analysis***:**

Molecular docking simulations were performed using AutoDock Vina within the PyRx platform [4]. Grid box parameters were defined to encompass the active binding sites of the receptors based on the coordinates of their co-crystallized ligands. Docking was carried out using default exhaustiveness settings to predict the binding affinities of the selected phytochemicals against the two receptors. Binding affinity values (kcal/mol) were recorded for each ligand–receptor interaction. The best docking pose for each compound was selected based on the lowest binding energy and favorable binding orientation. Visualization and interaction analysis of docked complexes were conducted using Discovery Studio Visualizer [14], focusing on hydrogen bonds, hydrophobic interactions, van der Waals forces, and other non-covalent interactions within the active site.

*2.2.5 Pharmacokinetic and Drug-Likeness Prediction***:**

Pharmacokinetic properties and drug-likeness of the selected phytochemicals were evaluated using the SwissADME and ADMETLAB web servers [11]. Parameters assessed included Lipinski's rule of five, gastrointestinal absorption, bioavailability score, and physicochemical properties relevant to oral drug development. Compounds that satisfied the recommended drug-likeness criteria were considered suitable candidates for further investigation.

2.2.6 Data Analysis

Docking scores were expressed as binding affinity values (kcal/mol). Comparative analysis was performed between the phytochemicals and the reference ligands originally co-crystallized with receptors 6DDF and 6DZZ. Compounds demonstrating stronger or comparable binding affinities and favorable interaction profiles were considered to possess higher predicted antidiarrhoeal potential.

2.3 Statistical Analysis

Docking scores were analyzed descriptively using binding affinity values expressed in kcal/mol. Comparative analyses between phytochemicals and reference ligands were conducted based on binding energies and interaction profiles.

3.0 RESULTS

3.1 Docking scores/binding affinities: The docking scores were obtained using PyRx and these scores were subjected to an elimination process to streamline the docking scores to those with similar or closer scores to those of the standards loperamide and alosetron.

Table 1**:** Binding Affinities of Phytoconstituents from *Vernonia amygdalina* against the target proteins

S/N	Compound Name	PUBCHEM ID	6DDF	6DZZ
1	MLS002703008	104830	-10.2	=
2	Stigmasteryl-Beta-D-Glucopyranoside	12895774	-8.7	-11.1
3	(8R,9R,13S,14R,17S)-13-methyl-6,7,8,9,11,12,14,15,16,17-decahydrocyclopenta[a]phenanthrene-3,17-diol	126969992	=	-10.1
4	3-[16-hydroxy-10,13-dimethyl-3-[3,4,5-trihydroxy-6-(hydroxymethyl)oxan-2-yl]oxy-2,3,4,5,6,12,14,15,16,17-decahydro-1H-cyclopenta[a]phenanthren-17-yl]-5-(3-methyl-2-propan-2-yloxiran-2-yl)oxolan-2-one	162858131	-9.4	-9.9
5	(3R,5S)-3-[(3S,5S,10S,13S,14R,16R,17R)-16-hydroxy-10,13-dimethyl-3-[(2R,3R,4S,5S,6R)-3,4,5-trihydroxy-6-(hydroxymethyl)oxan-2-yl]oxy-2,3,4,5,6,12,14,15,16,17-decahydro-1H-cyclopenta[a]phenanthren-17-yl]-5-[(2R,3S)-3-methyl-2-propan-2-yloxiran-2-yl]oxolan-2-one	162858132	-9.6	-10.7
6	(3R,5S)-3-[(3S,5S,10S,13S,14R,16S,17R)-16-hydroxy-10,13-dimethyl-3-[(2R,3R,4S,5S,6R)-3,4,5-trihydroxy-6-(hydroxymethyl)oxan-2-yl]oxy-2,3,4,5,6,12,14,15,16,17-decahydro-1H-cyclopenta[a]phenanthren-17-yl]-5-[(2R,3S)-3-methyl-2-propan-2-yloxiran-2-yl]oxolan-2-one	162858133	-9.6	-9.8
7	(3R,5S)-3-[(3S,5S,10S,13S,14R,17R)-10,13-dimethyl-16-oxo-3-[(2R,3R,4S,5S,6R)-3,4,5-trihydroxy-6-(hydroxymethyl)oxan-2-yl]oxy-1,2,3,4,5,6,12,14,15,17-decahydrocyclopenta[a]phenanthren-17-yl]-5-[(2R,3S)-3-methyl-2-propan-2-yloxiran-2-yl]oxolan-2-one	162894056	-9.5	-10.3
8	(3S,4R,5S)-3-[(3S,5S,10S,13R,14R,17R)-10,13-dimethyl-3-[(2R,3R,4S,5S,6R)-3,4,5-trihydroxy-6-(hydroxymethyl)oxan-2-yl]oxy-2,3,4,5,6,12,14,15,16,17-decahydro-1H-cyclopenta[a]phenanthren-17-yl]-4-hydroxy-5-[(2R,3S)-3-methyl-2-propan-2-yloxiran-2-yl]oxolan-2-one	162900761	-9.3	-10.3
9	[(1R,3S,4R,5S,8R,9Z,13R,15S)-15-hydroxy-5-methyl-6-oxo-7,14,16-trioxatetracyclo[8.4.3.01,13.04,8]heptadec-9-en-3-yl] 2-(hydroxymethyl)prop-2-enoate	162932203	=	-9.5
10	(3S,5R,9R,10S,13R,14R,17R)-17-[(2R)-5-ethyl-6-methylhept-5-en-2-yl]-10,13-dimethyl-2,3,4,5,6,9,11,12,14,15,16,17-dodecahydro-1H-cyclopenta[a]phenanthren-3-ol	163013902	=	-9.9
11	(2S)-4-[(3S,5S,10S,13S,14R,16R,17S)-3,16-dihydroxy-10,13-dimethyl-2,3,4,5,6,12,14,15,16,17-decahydro-1H-cyclopenta[a]phenanthren-17-yl]-2-[(2S,3R)-2,3-dihydroxy-4-methylpentan-3-yl]-2H-furan-5-one	163060310	-8.9	-10.7

12	[(1R,3S,4R,5S,8R,9Z,13R,15S)-15-hydroxy-5-methyl-6-oxo-7,14,16-trioxatetracyclo[8.4.3.01,13.04,8]heptadec-9-en-3-yl] 2-methylprop-2-enoate	163076706	=	-9.6
13	Vernodalin	179375	=	-9.6
14	Stigmasterol	5280794	-8.7	=
15	Poriferasterol	5281330	-8.8	-10.4
16	Chondrillasterol	5283663	-8.7	-10.8
17	Methaqualone	6292	=	-9.5
18	Squalene	638072	=	-9.7
19	Alpha-Amyrin Acetate	92842	-9.7	=

Table 2: Binding affinities of *Ocimum gratissimum* against the proposed targets.

S/N	Compound Name	PUBCHEM ID	6DDF	6DZZ
1	Tenuiorin	10391110	-8.6	-10.3
2	Cynaropicrin	119093	=	-9.5
3	Betulonic acid	122844	-9.4	-9.9
4	Taraxasterol acetate	13889352	-9.7	=
5	Isovitexin	162350	-8.6	-9.5
6	[3-hydroxy-4-(3-methoxy-4-methoxycarbonyl-5-methylphenoxy)carbonyl-5-methylphenyl] 2-hydroxy-4-methoxy-6-methylbenzoate	162845304	=	-10.1
7	(3S,4S)-3-[[(2S,3R)-7-hydroxy-2-(4-hydroxy-3-methoxyphenyl)-3-(hydroxymethyl)-2,3-dihydro-1-benzofuran-5-yl]methyl]-4-[(4-hydroxy-3-methoxyphenyl)methyl]oxolan-2-one	162855367	-8.9	-10.9
8	(3S,3aR,6S,6aS)-3-(3,4-dihydroxyphenyl)-6-(4-hydroxy-3,5-dimethoxyphenyl)-3,3a,6,6a-tetrahydro-1H-furo[3,4-c]furan-4-one	162953737	=	-9.5
9	(4aR,6aR,6aR,6bR,8aR,12S,12aS,14aR,14bR)-4,4,6a,6b,8a,12,14b-heptamethyl-11-methylidene-2,4a,5,6,6a,7,8,9,10,12,12a,13,14,14a-tetradecahydro-1H-picen-3-one	163035858	-9.1	=
10	[4-(3-hydroxy-4-methoxycarbonyl-5-methylphenoxy)carbonyl-3-methoxy-5-methylphenyl] 2-hydroxy-4-methoxy-6-methylbenzoate	163066241	-8.5	=
11	[3-methoxy-4-(3-methoxy-4-methoxycarbonyl-5-methylphenoxy)carbonyl-5-methylphenyl] 2-hydroxy-4-methoxy-6-methylbenzoate	163069661	=	-9.9
12	(1S,3aR,5aR,5bR,7aS,11aS,11bS,13aS,13bS)-3a,5a,5b,8,8,11a-hexamethyl-1-propan-2-yl-2,3,4,5,6,7,7a,11b,12,13,13a,13b-dodecahydro-1H-cyclopenta[a]chrysen-11-one	163193880	-10	=
13	Stigmast-5-en-3-ol	22012	-8.8	-11.2
14	Beta-Sitosterol	222284	-8.9	-11.1
15	Lupeol	259846	-10.6	=
16	Apigetrin	5280704	-9	=
17	Stigmasterol	5280794	-8.9	-10.3
18	Nepetoidin A	5316820	-8.5	=
19	Daucosterol	5742590	-8.9	-10.4
20	Ethinyl estradiol	5991	=	-9.7
21	3-Hydroxyolean-12-en-28-oic acid	619166	-9.2	=
22	Ursolic acid	64945	-9.2	=
23	Beta-Amyrin	73145	-10.2	=

Table 3: Binding affinities of *Piper guineense* against the proposed targets.

S/N	Compound Name	PUBCHEM ID	6DDF	6DZZ
1	(1R,2R,4aS,8aS)-2-(1,3-benzodioxol-5-yl)-N-(2-methylpropyl)-1,2,4a,5,6,7,8,8a-octahydronaphthalene-1-carboxamide	101821165	-8.5	=
2	[(1R,2S,4aR,8aS)-2-(1,3-benzodioxol-5-yl)-1,2,4a,5,6,7,8,8a-octahydronaphthalen-1-yl]-piperidin-1-ylmethanone	11035962	-9.1	-9.6
3	Cubebin	117443	=	-10.5
4	[(1S,2S,4aR,8aR)-2-(1,3-benzodioxol-5-yl)-1,2,4a,5,6,7,8,8a-octahydronaphthalen-1-yl]-piperidin-1-ylmethanone	11783540	-9.6	=
5	O-Ethylcubebin	13939336	=	-10.4
6	(2S,3S,4S)-3,4-bis(1,3-benzodioxol-5-ylmethyl)oxolan-2-ol	14137604	=	-9.9
7	[(1R,2R,4aS,8aS)-2-(1,3-benzodioxol-5-yl)-1,2,4a,5,6,7,8,8a-octahydronaphthalen-1-yl]-pyrrolidin-1-ylmethanone	162951652	-9	-10
8	[(1R,2S,4aS,8aS)-2-(1,3-benzodioxol-5-yl)-1,2,4a,5,6,7,8,8a-octahydronaphthalen-1-yl]-pyrrolidin-1-ylmethanone	162951653	-8.7	-10
9	5-[[(2S,3S,4S)-4-(1,3-benzodioxol-5-ylmethyl)-2-ethoxyoxolan-3-yl]methyl]-1,3-benzodioxole	162953580	=	-9.9
10	Campesterol	173183	-8.9	-10.3
11	Beta-Sitosterol	222284	-8.4	-9.9
12	Rac-Cubebin	287685		-9.6
13	Hinokinin	442879	-8.6	-9.7
14	Beta-Carotene	5280489	=	-9.8
15	Stigmasterol	5280794	-9.2	-11.1
16	23,24-Dihydrocucurbitacin F	54747446	-9	=
17	5-[(3R,3aS,6S,6aR)-3-(1,3-benzodioxol-5-yl)-1,3,3a,4,6,6a-hexahydrofuro[3,4-c]furan-6-yl]-1,3-benzodioxole	7059611	-8.7	-10.8
18	Sesamin	72307	-8.7	-10.8

Table 4: Binding affinities of standard ligands against the proposed targets.

S/N	COMPOUND NAME	PUCHEM ID	6DDF	6DZZ
1	Loperamide	3955	-8.4	=
2	Alosetron	2099	=	-9.5

3.2 ADME analysis

Table 5: ADME Profiling of ligands from *Vernonia amygdalina.*

S/N	PubChem ID	Molecular Weight	No of Hydrogen Acceptors	No of Hydrogen Donors	Consensus Log P	Lipinski Violations
1	104830	502.55	9	1	2.29	1
2	12895774	574.83	6	4	5.22	1
3	126969992	272.38	2	2	3.4	0
4	162858131	632.78	10	5	2.38	1
5	162858132	632.78	10	5	2.47	1
6	162858133	632.78	10	5	2.53	1
7	162894056	630.77	10	4	2.53	1
8	162900761	632.78	10	5	2.68	1
9	162932203	380.39	8	2	0.74	0

10	163013902	412.69	1	1	7.08	1
11	163060310	486.64	6	4	3.17	0
12	163076706	364.39	7	1	1.5	0
13	179375	360.36	7	1	1.48	0
14	5280794	412.69	1	1	6.98	1
15	5281330	412.69	1	1	6.98	1
16	5283663	412.69	1	1	6.96	1
17	6292	250.3	2	0	2.96	0
18	638072	410.72	0	0	2.96	0
19	92842	468.75	2	0	7.49	1

Table 6: ADME Profiling of ligands from *Ocimum gratissimum.*

S/N	PubChem ID	MW	No of Hydrogen Acceptors	No of Hydrogen Donors	Consensus Log P	Lipinski Violations
1	10391110	496.46	10	3	4.04	0
2	119093	346.37	6	2	1.41	0
3	122844	454.68	3	1	6.17	1
4	13889352	468.75	2	0	7.51	1
5	162350	432.38	10	7	-0.02	1
6	162845304	510.49	10	2	4.25	1
7	162855367	522.54	9	4	3.21	1
8	162953737	388.37	8	3	1.62	0
9	163035858	424.7	1	0	7.14	1
10	163066241	510.49	10	2	4.32	1
11	163069661	524.52	10	1	4.57	1
12	163193880	424.7	1	0	7.26	1
13	22012	414.71	1	1	7.23	1
14	222284	414.71	1	1	7.24	1
15	259846	426.72	1	1	7.27	1
16	5280704	432.38	10	6	0.52	1
17	5280794	412.69	1	1	6.98	1
18	5316820	314.29	6	4	2.16	0
19	5742590	576.85	6	4	5.55	1
20	5991	296.4	2	2	3.63	0
21	619166	456.7	3	2	6.06	1
22	64945	456.7	3	2	5.93	1
23	73145	426.72	1	1	7.16	1

Table 7: ADME Profiling of ligands from *Piper guineense.*

S/N	PubChem ID	MW	No of Hydrogen Acceptors	No of Hydrogen Donors	Consensus Log P	Lipinski Violations
1	101821165	355.47	3	1	4.15	0
2	11035962	367.48	3	0	4.06	0
3	117443	356.37	6	1	2.98	0
4	11783540	367.48	3	0	4.09	0
5	13939336	384.42	6	0	3.72	0
6	14137604	356.37	6	1	2.9	0
7	162951652	353.45	3	0	3.78	0
8	162951653	353.45	3	0	3.77	0

9	162953580	384.42	6	0	3.72	0
10	173183	400.68	1	1	6.92	1
11	222284	414.71	1	1	7.24	1
12	287685	356.37	6	1	2.9	0
13	442879	354.35	6	0	3.24	0
14	5280489	536.87	0	0	3.24	0
15	5280794	412.69	1	1	6.98	1
16	54747446	520.7	7	5	2.58	1
17	7059611	354.35	6	0	2.79	0
18	72307	354.35	6	0	2.79	0

3.3 Toxicity analysis

The toxicity profile of these compounds was obtained by inputting the SMILES of the compound gotten from PUBCHEM into ADMETLAB.

Table 8: Toxicity prediction of Ligands from *Vernonia amygdalina.*

S/N	PubChem ID	Carcinogenicity	Respiratory	Neurotoxicity-DI	Ototoxicity	Hematotoxicity	Nephrotoxicity-DI
1	104830	0.5163	0.1259	0.7141	0.8555	0.4380	0.9664
2	12895774	0.4520	0.1354	0.0055	0.9572	0.5723	0.5940
3	126969992	0.9422	0.9023	0.1113	0.6002	0.2304	0.1888
4	162858131	0.0683	0.0142	0.6568	0.9993	0.0274	0.0831
5	162858132	0.4380	0.0913	0.0600	0.9808	0.6541	0.8842
6	162858133	0.3835	0.0857	0.0724	0.9898	0.6411	0.8601
7	162894056	0.3755	0.0544	0.1253	0.9869	0.8312	0.9207
8	162900761	0.1474	0.0504	0.0097	0.9892	0.5331	0.7336
9	162932203	0.2580	0.3654	0.1619	0.8853	0.4443	0.8586
10	163013902	0.8158	0.8838	0.0668	0.3338	0.4457	0.4822
11	163060310	0.9727	0.6950	0.2655	0.5369	0.3087	0.9414
12	163076706	0.2075	0.5227	0.2720	0.8336	0.4145	0.8312
13	179375	0.9504	0.3434	0.7164	0.7519	0.8158	0.9202
14	5280794	0.8748	0.9396	0.1569	0.5748	0.4538	0.5464
15	5281330	0.7854	0.6997	0.0396	0.6048	0.3474	0.5068
16	5283663	0.7634	0.7921	0.0223	0.6437	0.5565	0.6372
17	6292	0.6948	0.7447	0.9173	0.3367	0.4940	0.3771
18	638072	0.0238	0.9862	0.6211	0.3918	0.3411	0.5950
19	92842	0.8876	0.5503	0.0562	0.2519	0.5654	0.3867

Table 9: Toxicity prediction of Ligands from *Ocimum gratissimum.*

S/N	PubChem ID	Carcinogenicity	Respiratory	Neurotoxicity-DI	Ototoxicity	Hematotoxicity	Nephrotoxicity-DI
1	10391110	0.4269	0.8072	0.0964	0.1711	0.0150	0.1760
2	119093	0.8604	0.4831	0.8427	0.8309	0.8194	0.8541
3	122844	0.9283	0.9142	0.1328	0.4744	0.6417	0.7731
4	13889352	0.9137	0.7568	0.2321	0.2751	0.6898	0.7506
5	162350	0.2878	0.0684	0.0060	0.6226	0.0647	0.1049
6	162845304	0.4974	0.7252	0.2237	0.2129	0.0458	0.3084
7	162855367	0.4522	0.1866	0.4134	0.8905	0.5847	0.9192
8	162953737	0.3973	0.2414	0.1555	0.4892	0.2484	0.2439
9	163035858	0.8708	0.8019	0.5640	0.4046	0.8203	0.7943

10	163066241	0.5309	0.7418	0.2399	0.1896	0.0320	0.2447
11	163069661	0.6047	0.6449	0.4609	0.2390	0.0965	0.4141
12	163193880	0.9363	0.9085	0.2162	0.4112	0.6979	0.8935
13	22012	0.5379	0.9215	0.1769	0.5715	0.3476	0.4474
14	222284	0.6884	0.8728	0.0933	0.4836	0.2604	0.4602
15	259846	0.9323	0.9175	0.1142	0.3905	0.5577	0.6601
16	5280704	0.4716	0.0359	0.0031	0.7668	0.1248	0.3466
17	5280794	0.8748	0.9396	0.1569	0.5748	0.4538	0.5464
18	5316820	0.4955	0.0715	0.0346	0.3186	0.0082	0.0596
19	5742590	0.3325	0.3161	0.0137	0.9320	0.4699	0.5484
20	5991	0.9049	0.9979	0.6296	0.8210	0.0061	0.3168
21	619166	0.1704	0.7423	0.1641	0.9129	0.1489	0.1501
22	64945	0.9192	0.9390	0.0516	0.5728	0.5840	0.8734
23	73145	0.9127	0.8459	0.1854	0.4166	0.5284	0.7313

Table 10: Toxicity prediction of Ligands from *Piper guineense.*

S/N	PubChem ID	Carcinogenicity	Respiratory	Neurotoxicity-DI	Ototoxicity	Hematotoxicity	Nephrotoxicity-DI
1	101821165	0.8185	0.4844	0.0823	0.2806	0.5703	0.3890
2	11035962	0.6997	0.7616	0.5161	0.3309	0.3888	0.3406
3	117443	0.5294	0.6657	0.7064	0.7902	0.4468	0.8764
4	11783540	0.4053	0.6048	0.5823	0.3355	0.3747	0.4372
5	13939336	0.5677	0.5761	0.6573	0.8289	0.3752	0.5674
6	14137604	0.7236	0.4765	0.8164	0.7171	0.4172	0.8616
7	162951652	0.8171	0.7699	0.1434	0.2212	0.6099	0.5028
8	162951653	0.7473	0.7558	0.2216	0.3191	0.5879	0.5224
9	162953580	0.7464	0.3674	0.8160	0.5091	0.4561	0.8346
10	173183	0.8749	0.7985	0.0658	0.4236	0.2966	0.4672
11	222284	0.6884	0.8728	0.0933	0.4836	0.2604	0.4602
12	287685	0.5352	0.5844	0.7194	0.9333	0.3530	0.5942
13	442879	0.9206	0.2247	0.8531	0.6087	0.7317	0.9155
14	5280489	0.8052	0.8173	0.6096	0.6847	0.5190	0.8246
15	5280794	0.8748	0.9396	0.1569	0.5748	0.4538	0.5464
16	54747446	0.6308	0.3889	0.0425	0.8610	0.4776	0.6400
17	7059611	0.8778	0.3973	0.3738	0.2084	0.5867	0.5520
18	72307	0.9032	0.4019	0.5439	0.2656	0.4870	0.6301

3.4 Ligand Interactions

Molecular interaction analysis with 6DZZ and 6DDF receptors.

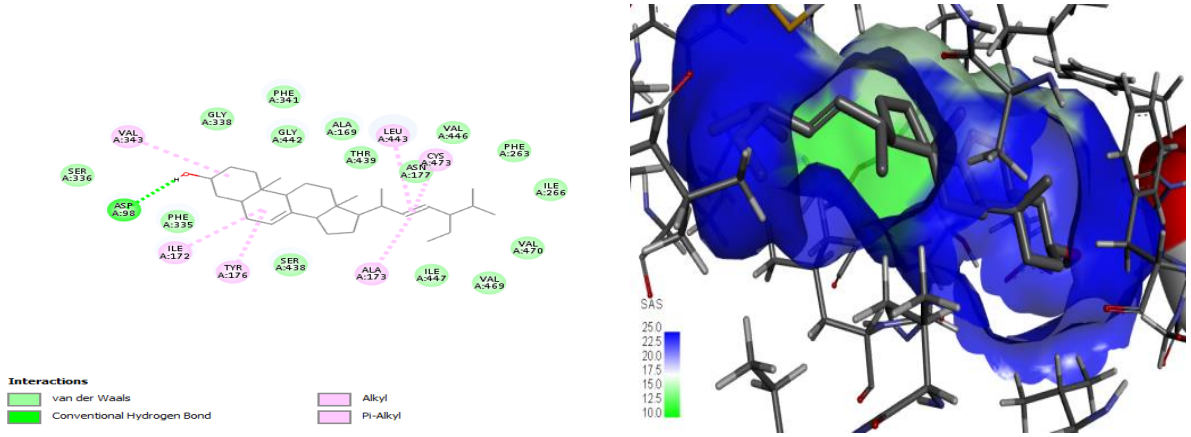

Figure 1: Two-dimensional and three-dimensional interaction profile of PubChem ID 5283663 with the serotonin transporter (6DZZ) showing hydrogen bonding and hydrophobic interactions.

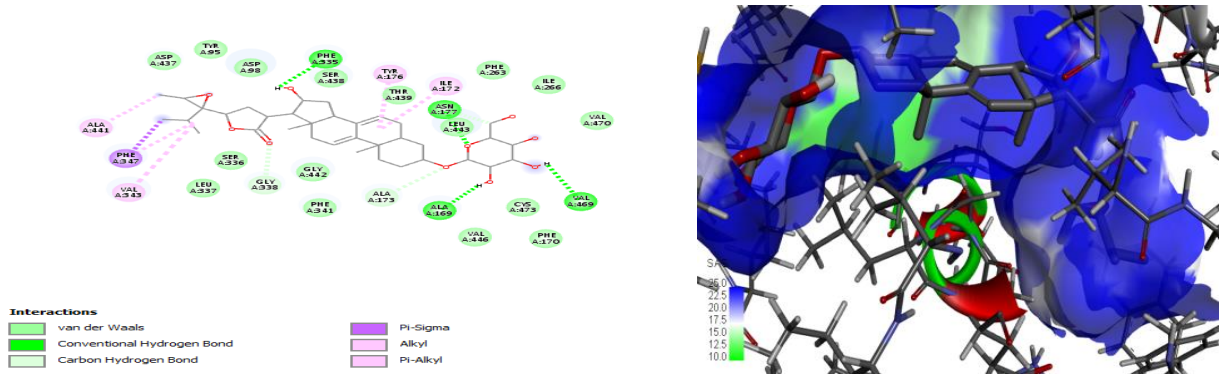

Figure 2: Two-dimensional and three-dimensional interaction profile of PubChem ID 162858131 with the serotonin transporter (6DZZ) showing hydrogen bonding and hydrophobic interactions.

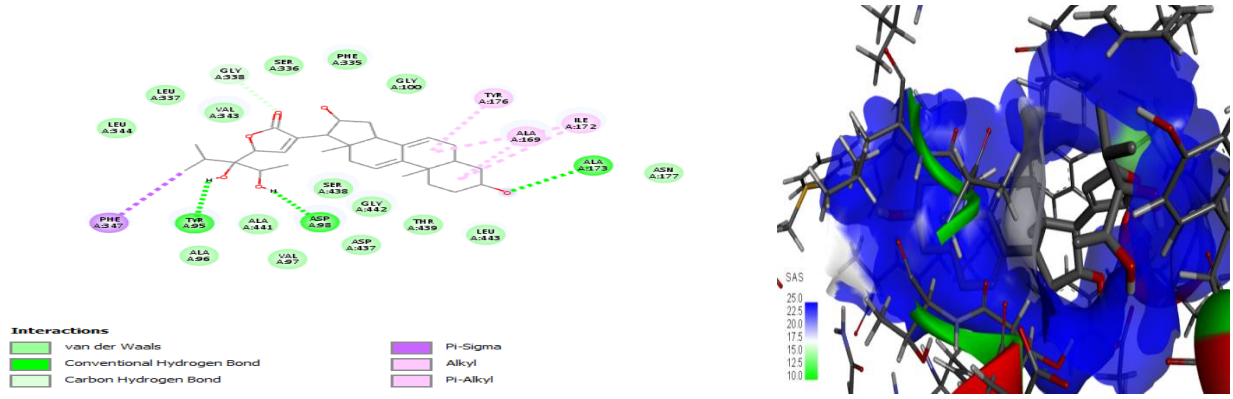

Figure 3: Two-dimensional and three-dimensional interaction profile of PubChem ID 163060310 with the serotonin transporter (6DZZ) showing hydrogen bonding and hydrophobic interactions.

Nigerian Journal of Pharmaceutical and Applied Science Research,
Vol.15 (2): 7-22; June 2026 *ISSN: 2971-737X (Print); ISSN: 2971-7388.*
Available at www.nijophasr.net *https://doi.org/10.60787/nijophasr-v15-i2-649*

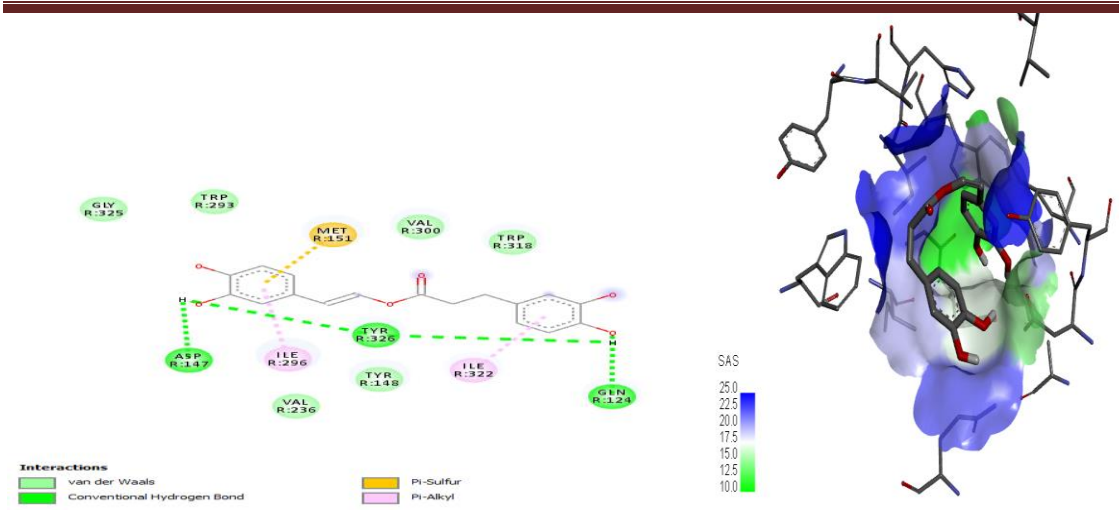

Figure 4: Two-dimensional and three-dimensional interaction profile of PubChem ID 5316820 with the mu receptor (6DFF) showing hydrogen bonding and hydrophobic interactions.

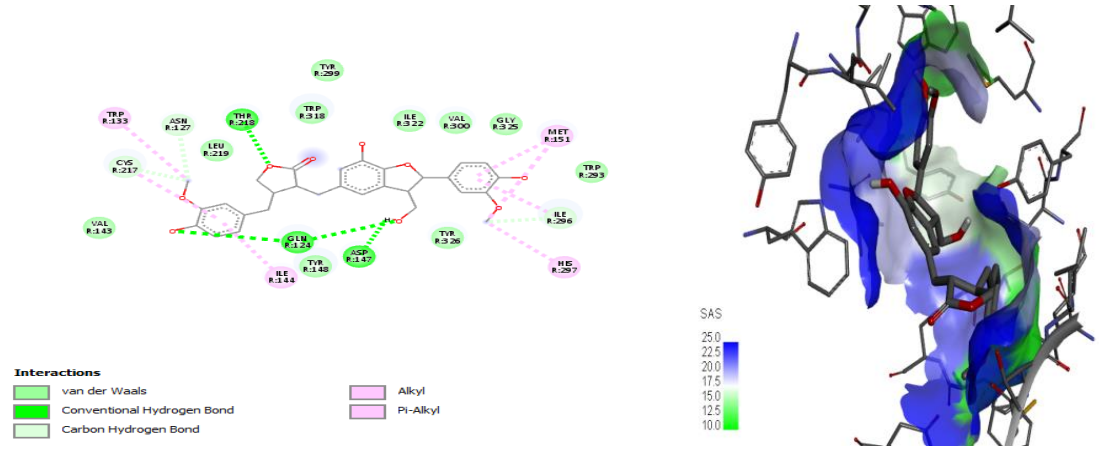

Figure 5: Two-dimensional and three-dimensional interaction profile of PubChem ID 162855367 with the mu receptor (6DFF) showing hydrogen bonding and hydrophobic interactions.

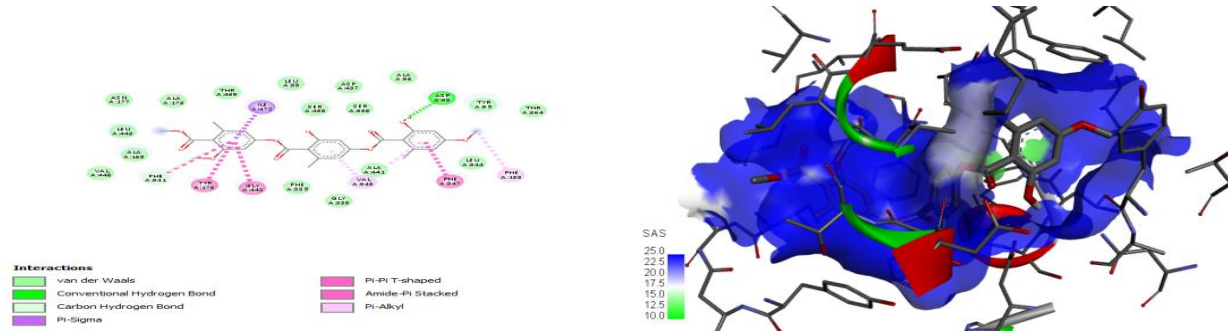

Figure 6: Two-dimensional and three-dimensional interaction profile of PubChem ID 162845304 with the serotonin transporter (6DZZ) showing hydrogen bonding and hydrophobic interactions.

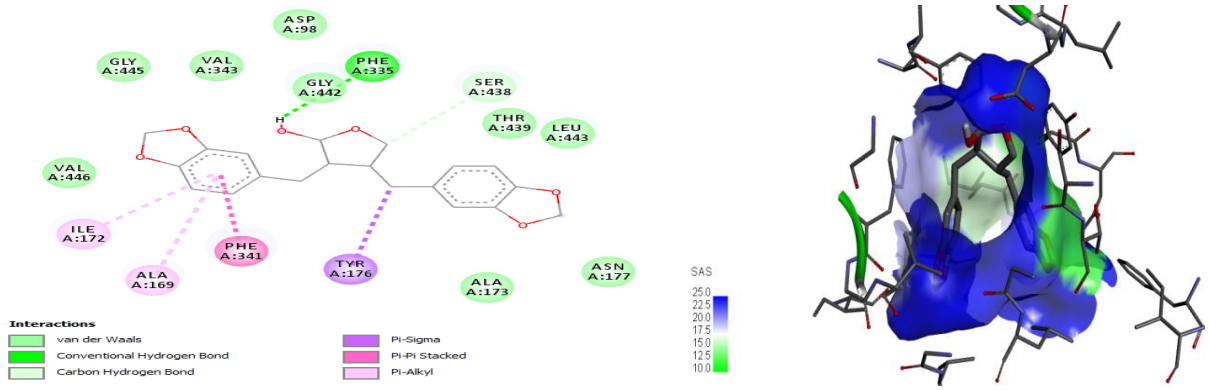

Figure 7: Two-dimensional and three-dimensional interaction profile of PubChem ID 287685 with the serotonin transporter (6DZZ) showing hydrogen bonding and hydrophobic interactions.

4.0 DISCUSSION

The molecular docking results obtained in this study provide insight into the binding affinities and interaction profiles of selected phytoconstituents from *Vernonia amygdalina*, *Ocimum gratissimum*, and *Piper guineense* against key protein targets implicated in diarrhoeal pathophysiology. Computational docking has become an established approach for predicting ligand–receptor interactions and identifying bioactive compounds with therapeutic potential prior to experimental validation [15,16]. The comparative analysis of binding energies, hydrogen bonding, and hydrophobic interactions observed in this study offers a mechanistic basis for the antidiarrhoeal claims associated with these vegetables in traditional diets and ethnomedicine [17,18]. Furthermore, the integration of drug-likeness and pharmacokinetic predictions strengthens the identification of lead compounds with favorable therapeutic prospects [11]. The findings are discussed in relation to standard antidiarrhoeal agents and existing structure-activity evidence.

4.1 Justification of Positive Controls

The use of positive controls in molecular docking studies provides a reference for evaluating the binding potential of test compounds against validated therapeutic targets. In this study, loperamide and alosetron were selected as standard ligands for the μ-opioid receptor (6DDF) and human serotonin transporter (6DZZ), respectively, due to their established relevance in the management of diarrhoeal disorders. Loperamide was selected as the reference ligand for 6DDF because it is a clinically approved antidiarrhoeal drug that acts through activation of peripheral μ-opioid receptors in the gastrointestinal tract. Its mechanism involves reduction of intestinal motility, inhibition of fluid secretion, and increased water absorption, thereby improving diarrhoeal symptoms [2,3]. Since the μ-opioid receptor is a major target mediating the pharmacological effects of loperamide, its inclusion provides an appropriate benchmark for comparing the binding affinities and interaction profiles of the phytoconstituents. Alosetron was selected as the positive control for 6DZZ due to its established role in the management of diarrhea-predominant irritable bowel syndrome (IBS-D), where excessive serotonin signaling contributes to increased intestinal motility and secretion [5]. Although primarily a 5-HT_3 receptor antagonist, alosetron modulates serotonergic pathways involved in gastrointestinal function. Therefore, its use as a reference ligand provides a pharmacologically relevant basis for evaluating phytoconstituent interactions with serotonin-associated mechanisms represented by the serotonin transporter. The inclusion of these standard ligands strengthens the reliability of the docking analysis by allowing comparison of phytoconstituent binding affinities with clinically relevant antidiarrhoeal agents. Compounds with binding scores comparable to or better than the standards may therefore possess promising antidiarrhoeal potential. This study uses Loperamide and Alosetron as the control or standard ligands for 6DDF and 6DZZ respectively. The Mu Opioid Receptor-Gi Protein Complex was shown to have 16 amino acid residues in its binding pocket according to visualization studies carried out in PyMOL. The key amino acid residues responsible for its activity identified to be ASP-147 from literature [19,20]. The Cryo-EM Structure of the wild-type human serotonin transporter in complex with ibogaine and 15B8 Fab in the inward conformation was shown to have ibogaine binding to 19 amino acid residues according to visualization studies carried out using PyMOL with the key amino acid residues responsible for its activity identified to be ASP-98 and PHE-335. The binding affinities of the control ligands are -8.4 (6DDF) and -9.5

(6DZZ). In this study, attention was focused on the test ligands which interacted with the active sites of the various proteins, as well as the type of molecular bond with the active site, in addition to possessing binding affinities equal to or lower than those of the control ligands. Several phytochemicals from *Vernonia amygdalina* demonstrated remarkable binding affinities against both targets (Table 1). Notably, MLS002703008 (PubChem ID: 104830) exhibited a binding affinity of −10.2 kcal/mol against 6DDF, substantially stronger than loperamide. Stigmasteryl-β-D-glucopyranoside (PubChem ID: 12895774) showed dual activity, with −8.7 kcal/mol against 6DDF and −11.1 kcal/mol against 6DZZ, outperforming both control ligands. Similarly, complex steroidal glycosides (PubChem IDs: 162858132, 162858133, 162894056) demonstrated strong interactions with the serotonin transporter, with binding energies ranging from −9.8 to −10.7 kcal/mol. Chondrillasterol (PubChem ID: 5283663) also showed significant affinity (−10.8 kcal/mol) toward 6DZZ. These findings suggest that steroidal frameworks may favor hydrophobic interactions within the transporter's binding cavity, potentially stabilizing conformations associated with reduced serotonergic hyperactivity in diarrhoeal. Interestingly, several Vernonia-derived compounds showed selectivity toward one target, suggesting possible differential modulation of intestinal motility versus serotonin-mediated secretion pathways. This selective interaction profile may be advantageous in reducing off-target effects. Phytoconstituents from *Ocimum gratissimum* also demonstrated strong binding interactions (Table 2). Tenuiorin (PubChem ID: 10391110) exhibited binding affinities of −8.6 kcal/mol (6DDF) and −10.3 kcal/mol (6DZZ), while Betulonic acid (PubChem ID: 122844) showed −9.4 kcal/mol (6DDF) and −9.9 kcal/mol (6DZZ), both comparable and superior to the reference ligands. Notably, compound 162855367 demonstrated −10.9 kcal/mol against 6DZZ, representing one of the strongest interactions observed in this study. Taraxasterol acetate (PubChem ID: 13889352) showed −9.7 kcal/mol against 6DDF, exceeding loperamide's affinity. These triterpenoid and phenolic derivatives likely establish hydrophobic and van der Waals interactions within the receptor binding sites, potentially complemented by hydrogen bonding through hydroxyl substituents. The consistent high affinity of Ocimum-derived compounds toward the serotonin transporter suggests a potential mechanism involving modulation of serotonin reuptake, which may reduce excessive intestinal secretion and motility. Phytoconstituents from *Piper guineense* (Table 3) similarly demonstrated promising binding profiles. Several sterol derivatives exhibited affinities exceeding −9.5 kcal/mol against 6DZZ, while others showed competitive interaction with 6DDF. The presence of hydrophobic alkyl chains and steroidal cores in these compounds likely facilitates deep penetration into the hydrophobic regions of the receptor pockets. The ability of certain Piper-derived compounds to demonstrate strong dual-target affinity suggests potential multi-mechanistic antidiarrhoeal action—simultaneous modulation of opioid receptor–mediated motility suppression and serotonin transporter regulation. Across all three plants, numerous compounds exhibited binding affinities stronger than the standard ligands. Compounds achieving ≤ −10 kcal/mol may be considered strong binders in docking studies, suggesting stable ligand–receptor complex formation. The predominance of steroidal and triterpenoid scaffolds among high-affinity compounds indicates that lipophilic frameworks may favor binding within these gastrointestinal targets. Although docking scores do not directly equate to biological efficacy, stronger binding affinity relative to established drugs provides preliminary molecular justification for traditional ethnomedicinal use of these vegetables in managing diarrhoeal symptoms.

4.2 Drug-Likeness and Pharmacokinetic Considerations

SwissADME analysis revealed that several high-affinity compounds complied with Lipinski's Rule of Five, suggesting favorable oral bioavailability potential. However, certain glycosylated steroidal derivatives exceeded molecular weight thresholds (>500 Da) and may demonstrate limited absorption or solubility despite strong docking scores. Compounds with moderate molecular weight, acceptable logP values, and minimal Lipinski violations may represent more viable lead candidates for further development. Balancing binding strength with pharmacokinetic suitability is essential in early-stage drug discovery.

4.3 **Mechanistic Implications**

Activation of the Mu Opioid Receptor reduces intestinal motility and fluid secretion, while modulation of the serotonin transporter regulates serotonergic signaling implicated in diarrhoeal hypersecretion. The strong interaction of multiple phytoconstituents with ASP-147 (MOR) and ASP-98/PHE-335 (SERT) suggests that these compounds may influence receptor conformation and transporter function in a manner consistent with antidiarrhoeal pharmacodynamics. The dual-target activity observed among several compounds supports a poly-pharmacological mechanism, which may enhance therapeutic efficacy while reducing the likelihood of resistance or pathway compensation.

4.4 Toxicity Prediction of Selected Phytoconstituents

The toxicity assessment of phytoconstituents from *Vernonia amygdalina*, *Ocimum gratissimum*, and *Piper guineense* provided insight into the potential safety profile of the compounds identified as promising antidiarrhoeal candidates. Toxicity prediction is an important step in early drug discovery because compounds with strong binding affinity may still be unsuitable for therapeutic development if associated with high toxicity risks. In this study, toxicity endpoints including carcinogenicity, respiratory toxicity, neurotoxicity, ototoxicity, hematotoxicity, and nephrotoxicity were evaluated using ADMETLAB prediction models. The toxicity profile of compounds from *Vernonia amygdalina* (Table 8) showed considerable variation across toxicity endpoints. Several compounds, including PubChem IDs **162858131**, **162900761**, and **162932203**, demonstrated relatively low predicted carcinogenicity and respiratory toxicity, suggesting a comparatively favorable safety profile. However, some compounds such as **179375 (Vernodalin)** and **163060310** showed elevated carcinogenicity and nephrotoxicity scores, indicating the need for caution despite their favorable docking performance. High ototoxicity predictions were observed across many compounds, suggesting that toxicity risks may differ depending on organ-specific effects. For *Ocimum gratissimum* (Table 9), a number of phytoconstituents demonstrated comparatively lower predicted toxicity across multiple endpoints. Compounds such as **Isovitexin (162350)** and **Nepetoidin A (5316820)** exhibited low neurotoxicity, respiratory toxicity, hematotoxicity, and nephrotoxicity scores, suggesting improved safety potential. In contrast, compounds including **Betulonic acid (122844)**, **Lupeol (259846)**, and **Ursolic acid (64945)** displayed higher carcinogenicity and respiratory toxicity predictions, despite exhibiting strong docking affinities. These findings indicate that high receptor binding alone may not necessarily correspond to favorable safety outcomes. The toxicity predictions for *Piper guineense* phytoconstituents (Table 10) generally indicated moderate toxicity profiles. Several compounds, including **11783540** and **162951653**, exhibited relatively low toxicity across most evaluated parameters, making them potentially safer candidates for further investigation. Conversely, compounds such as **Hinokinin (442879)** and **Beta-carotene (5280489)** demonstrated elevated toxicity predictions for selected endpoints, particularly neurotoxicity and nephrotoxicity, which may limit their therapeutic suitability. Overall, the toxicity analysis revealed that several phytoconstituents with promising docking affinities also possessed acceptable predicted safety profiles, while others exhibited toxicity concerns that may restrict their pharmaceutical potential. Therefore, the selection of lead compounds should consider both molecular binding performance and toxicity outcomes to improve the likelihood of identifying safe and effective antidiarrhoeal candidates. Further **in vitro** and **in vivo** toxicological studies are necessary to validate these computational predictions.

4.5 Limitations

A limitation of this study is the reliance on computational prediction without experimental validation.

5.0 CONCLUSION

The study demonstrates that phytoconstituents from *Vernonia amygdalina*, *Ocimum gratissimum*, and *Piper guineense* possess significant *in silico* binding affinity toward key diarrhoeal-related molecular targets, in several cases exceeding that of standard antidiarrhoeal drugs. These findings provide molecular-level support for the traditional dietary and ethnomedicinal use of these plants in managing gastrointestinal disorders. Compounds combining strong docking affinity with favorable drug-likeness properties represent promising lead candidates for further pharmacological investigation.

5.1 Future Recommendations

Further *In vitro* and *In vivo* studies are recommended to validate the predicted antidiarrhoeal activities and safety profiles of these phytoconstituents.

DECLARATIONS

Acknowledgement

The authors sincerely acknowledge the Department of Pharmaceutical Chemistry, Faculty of Pharmacy, University of Benin, for providing the necessary resources and environment for this research.

Conflict of Interest

The authors affirm that none of their personal ties or known conflicts of interest might have influenced the work presented in this paper.

Author Contributions: Uyi M. Ogbeide conceptualized the study, supervised the research, and reviewed the manuscript. Kluvet O. Owowenu carried out *in silico* experiments, analyzed the data, and drafted the manuscript.

Ethical Approval

Ethical approval was not required for this study because no human participants or experimental animals were involved.

REFERENCES

[1] GBD Diarrhoeal Diseases Collaborators. Global, regional, and national burden of diarrhoeal diseases in 204 countries and territories, 1990–2019. Lancet Infectious Diseases. 2020;20(10):1185–1197.

[2] Holzer P. Opioid receptors in the gastrointestinal tract. Handbook of Experimental Pharmacology. 2019; 254:13–28.

[3] Wood JD, Galligan JJ. Function of opioids in the gastrointestinal tract. Handbook of Experimental Pharmacology. 2019; 254:71–90.

[4] Eberhardt J, Santos-Martins D, Tillack AF, Forli S. Molecular docking and structure-based drug design in modern pharmacology. Current Topics in Medicinal Chemistry. 2021;21(12):1017–1032.

[5] Kowalczyk A, Kalinowska M, Wroblewska A, et al. Serotonin in the gastrointestinal tract: physiological and pathological implications. Life. 2024;14(10):1280.

[6] Glatz F, Stiefl N, Rarey M. Ultra-large docking for the discovery of novel ligands targeting the serotonin transporter. Journal of Chemical Information and Modeling. 2023;63(12):3705–3717.

[7] Adeleye AO, Adebayo IA, Aremu AO, Femi-Oyewo MN. Antimicrobial and antispasmodic properties of *Ocimum gratissimum* essential oil: implications for gastrointestinal disorders. *Journal of* Ethnopharmacology. 2022; 289:115042.

[8] Nkeiruka EC, Okafor GI, Nwankwo IU. Phytochemical and pharmacological properties of *Piper guineense* and its potential therapeutic applications. African Journal of Biomedical Research. 2021;24(3):315–324.

[9] Farombi EO, Owoeye O. Antioxidant and anti-inflammatory effects of *Vernonia amygdalina*: therapeutic implications. Phytotherapy Research. 2019;33(9):2347–2359.

[10] Eberhardt J, Santos-Martins D, Tillack AF, Forli S. AutoDock Vina 1.2.0: new docking methods, expanded force field, and Python bindings. Journal of Chemical Information and Modeling. 2021;61(8):3891–3898.

[11] Daina A, Michielin O, Zoete V. SwissADME: a free web tool to evaluate pharmacokinetics, drug-likeness and medicinal chemistry friendliness of small molecules. Scientific Reports. 2017; 7:42717.

[12] Kim S, Chen J, Cheng T, Gindulyte A, He J, He S, et al. PubChem 2023 update: new data content and improved web interfaces. Nucleic Acids Research. 2023;51(D1): D1373–D1380.

[13] Burley SK, Bhikadiya C, Bi C, Bittrich S, Chen L, Crichlow GV, et al. RCSB Protein Data Bank: powerful new tools for exploring 3D structures of biological macromolecules. Nucleic Acids Research. 2021;49(D1): D437–D451.

[14] BIOVIA. *Discovery Studio Visualizer*, version 21.1. San Diego: Dassault Systèmes; 2021.

[15] Meng XY, Zhang HX, Mezei M, Cui M. Molecular docking: a powerful approach for structure-based drug discovery. Current Computer-Aided Drug Design. 2011;7(2):146–157.

[16] Pinzi L, Rastelli G. Molecular docking: shifting paradigms in drug discovery. International Journal of Molecular Sciences. 2019;20(18):4331.

[17] Ekor M. The growing use of herbal medicines: issues relating to adverse reactions and challenges in monitoring safety. Frontiers in Pharmacology. 2014; 4:177.

[18] Gyebi GA, Ogunyemi OM, Ibrahim IM, Afolabi SO. In silico screening of phytochemicals from Nigerian medicinal plants as potential inhibitors of angiotensin-converting enzyme. The Journal of Biomolecular Structure and Dynamics. 2021;39(16):5875–5886.

[19] Kaserer T, Lantero A, Schmidhammer H, Spetea M, Schuster D. Structure-based approach to rationalize the molecular interactions of μ-opioid receptor ligands. Scientific Reports. 2016;6: 21548..

[20] Manglik A, Kruse AC, Kobilka TS, Thian FS, Mathiesen JM, Sunahara RK, et al. Crystal structure of the μ-opioid receptor bound to a morphinan antagonist. Nature. 2012;485(7398):321–326.

[21] World Health Organization. Diarrhoeal disease fact sheet. Geneva: World Health Organization; 2023. Available from: https://www.who.int/news-room/fact-sheets/detail/diarrhoeal-disease. Accessed 15 September 2025.